ChemSusChem

Research Article
doi.org/10.1002/cssc.202401636

Chemistry Europe
European Chemical Societies Publishing

www.chemsuschem.org

VIP *Very Important Paper*

Glycerol Carbonate and Solketal Carbonate as Circular Economy Bricks for Supercapacitors and Potassium Batteries

Prisco Prete[+],[a] Sabrina Trano[+],[b] Pietro Zaccagnini[+],[b] Lucia Fagiolari,[b] Julia Amici,[b] Andrea Lamberti,[b] Antonio Proto,[a] Federico Bella,*[b] and Raffaele Cucciniello*[a]

Considering the worldwide market of batteries and supercapacitors, the (partial or total) replacement of conventional fossil-derived carbonates with bio-based ones in electrolyte formulations would allow the production of safer and more sustainable devices. In this work, embracing the 7th principle of green chemistry, glycerol derivatives (namely glycerol carbonate and solketal carbonate) are tested as solvents and additives for electrolyte formulations. Glycerol carbonate is innovatively employed as promising electrolyte solvent for electric double-layer capacitors with excellent performances. On the other hand, a solketal carbonate-laden liquid electrolyte is investigated for potassium-based batteries, showing a rather stable electrochemical behaviour and performance close to those of commercial oil-derived alternatives.

1. Introduction

The preparation of value-added chemicals from renewables is among the most investigated topics within the green chemistry and engineering community.[1–3] As a matter of fact, this approach is a clear repercussion of the 7th principle of green chemistry, which involves the use of bio-based feedstocks instead of fossil-derivatives.[4,5] In this scenario, among the plethora of chemicals obtained from renewables, an increasing interest has been devoted to those obtained through glycerol conversion, in the so-called glycerochemistry sector.[6,7] It is well-known that the huge amount of glycerol on market (5 billion liters in 2021 and expected to increase by 3% per year between 2021 and 2030[8,9]) is obtained as the main by-product of the bio-diesel industry at 10 wt%.[8,9] Therefore, it looks evident that glycerol will represent one of the major worldwide drop-in chemicals for the near future.[10]

In this context, several processes for glycerol valorization have been considered, including the preparation of solketal, oligomers and polymers, lactic acid, acrolein, citric acid, 1,3-propanediol, anti-freezing products, and others.[8,11] As a matter of fact, the use of glycerol-derived polymers, poly(ethoxyethyl glycidyl ether) and poly(glycidyl methyl ether), has recently been reported for sodium-based batteries by our research groups with interesting results.[12]

The vigorous advancement of bioderived, biosourced, or waste-derived materials intersects with another equally strategic sector, that is, the energy transition based on technologies (mainly electrochemical) to be used on a large scale to allow the conversion and storage of energy.[13–15] Regarding the latter point, the scientific community is intensely working on rechargeable batteries and supercapacitors; batteries can provide ≈10 times more energy than supercapacitors over longer periods of time (*i.e.*, higher specific energy),[16,17] while supercapacitors can deliver energy ≈10 times quicker than batteries (*i.e.*, higher specific power).[18,19] Different chemistries and devices have been explored in the field of supercapacitors and batteries, and this article focuses on two of these. First, electric double-layer capacitors (EDLCs) are symmetrical cells with a working mechanism based on the physical adsorption and desorption of ions at the carbon electrode/electrolyte interface.[20–22] Second, potassium-ion batteries (PIBs) are rechargeable cells based on the reversible intercalation (or insertion) of K^+ ions in various kinds of anodes and cathodes; with respect to their well-known lithium-based counterparts, PIBs are emerging for large-scale stationary applications, due to the wide potassium abundance and its cheapness, higher ion mobility due to the smaller Stokes' radius, and compatibility with aluminum current collectors (*i.e.*, cheaper and lighter than copper ones, typically used in lithium-ion batteries).[23,24] Both EDLCs and PIBs require an electrolyte system capable of quickly conducting ions between the electrodes, ensuring stability within the potential window in which these devices operate,

[a] *Department of Chemistry and Biology "Adolfo Zambelli", University of Salerno, Fisciano, Italy*
[b] *Department of Applied Science and Technology, Politecnico di Torino, Torino, Italy*

***Correspondence:** Raffaele Cucciniello, Department of Chemistry and Biology "Adolfo Zambelli", University of Salerno, Via Giovanni Paolo II 132, 84084 Fisciano, Italy.*
Email: rcucciniello@unisa.it

Federico Bella, Department of Applied Science and Technology, Politecnico di Torino, Corso Duca degli Abruzzi 24, 10129 Torino, Italy.
Email: federico.bella@polito.it

[+] *These authors contributed equally to the work.*

Supporting Information for this article is available on the WWW under https://doi.org/10.1002/cssc.202401636

also being durable for the entire life of the product.[25–27] These performances are normally obtained with electrolytes based on organic solvents of petrochemical origin (*e.g.* cyclic and linear carbonates or ethers), the environmental impact and safety requirements of which are currently at the center of the attention of the scientific community.[28,29] Their (partial or total) replacement with alternative solvents would allow the production of safer and more sustainable batteries and supercapacitors.

This work is focused on the synthesis and the innovative application of two chemicals obtained through glycerol catalytic conversion, *i.e.* glycerol carbonate (GlyC, 4-hydroxymethyl-2-oxo-1,3-dioxolane) and solketal carbonate (SLC, bis[(2,2-dimethyl-1,3-dioxolan-4-yl)methyl]carbonate)). Among glycerol-derived compounds, GlyC has raised an increasing interest in the last years due to its chemical-physical properties, which characterize this wide reactive molecule as a green starting compound for organics synthesis.[30] GlyC synthesis has been intensively investigated and different methodologies were reported in literature.[31] Due to its high boiling point (*i.e.*, 353.9 °C at 1 atm), GlyC and its derivates are considered potential candidate as low volatile organic compounds for many applications. Moreover, due to its high dielectric constant and dipole moment, GlyC is a good candidate as a solvent for electrolytes to be used in electrochemical energy storage devices.[32] On the other hand, SLC can be obtained by solketal (2,2-dimethyl-1,3-dioxolane-4-methanol) transesterification (*i.e.*, carbonate interchange reaction, CIR) with diethylcarbonate catalyzed by sodium methoxide (CH_3ONa), and it was formerly tested as lubricant.[33] The preparation of SLC involves a two steps reaction, where initially solketal is produced through glycerol acetalization in the presence of acetone (using both homogeneous or heterogeneous catalysts), and then used as starting material in the CIR.[34]

In this work, electrolytes for EDLCs and PIBs have been formulated with both GlyC and SLC, and their electrochemical behavior has been characterized along with the fabrication of lab-scale prototypes. The general trend observed shows the suitability of these compounds in the field of electrochemical energy storage, thus managing to reduce in these devices the amount/number of solvents derived from petrochemistry, *i.e.* a relevant milestone for these technologies upon which the energy and ecological transitions are based.

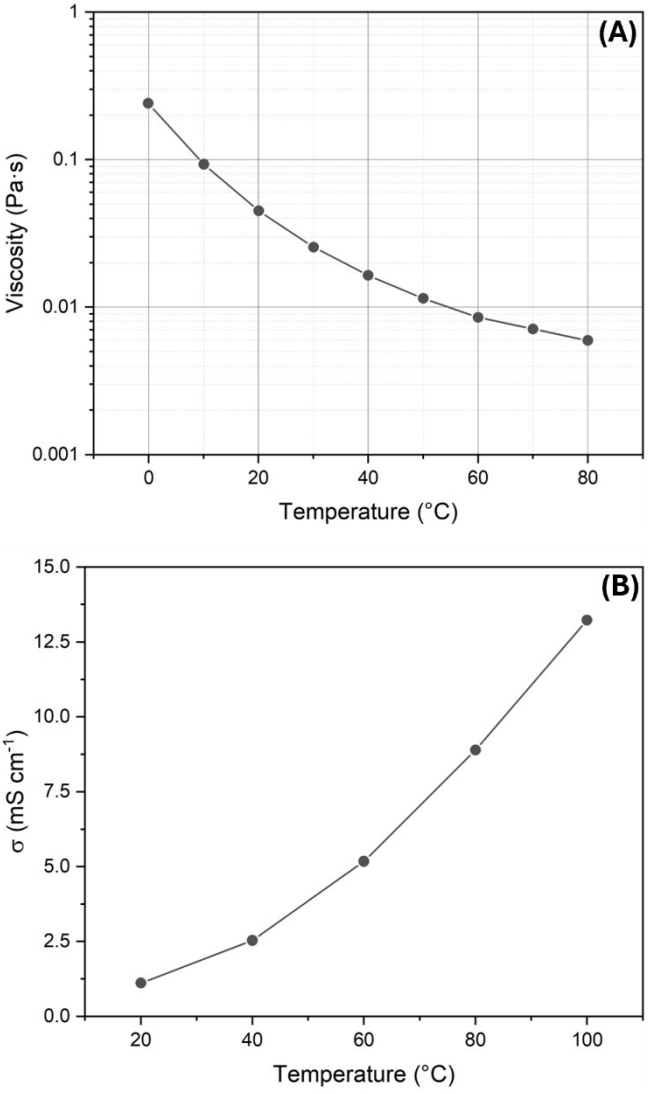

Figure 1. (A) Viscosity data for the GlyC-based electrolyte, analysed between 0 and 80 °C. **(B)** Ionic conductivity data for the same electrolyte, measured between 20 and 100 °C.

Results and Discussion

Glycerol Carbonate for Supercapacitors Electrolyte

Figure 1B shows the ionic conductivity values of the GlyC-based electrolyte upon temperature variation; the trend matches with the one obtained from rheological measurements (Figure 1A), *i.e.* when the temperature rises, the viscosity decreases and the ionic conductivity increases. Overall, the ionic conductivity at room temperature was lower if compared to typically obtained values of state-of-the-art electrolytes for supercapacitors,[21] *e.g.* propylene carbonate (PC)-based. This can be explained by considering the high electrolyte viscosity due to the use of GlyC as a solvent. Anyway, by increasing the temperature, the electrolyte viscosity hugely falls, reaching values analogous to those reported in the literature for conventional PC-based systems at ambient temperature. In particular, the electrolyte containing tetraethylammonium-tetrafluoroborate ($TEABF_4$) salt 1.0 M in GlyC reached $\approx$9 mS cm^{-1} and 6 mPa s at 80 °C, whereas the electrolyte adopting PC as a solvent displayed $\approx$10.5 mS cm^{-1} and 4 mPa s at room temperature.[35] Anyway, despite the not outstanding transport properties, the GlyC-based electrolyte displayed a rather good electrochemical behaviour when interfaced with carbon-based electrodes in a EDLC device, as outlined below, making it a promising candidate for sustainable capacitive energy storage.

Three-electrodes electrochemical measurements (*i.e.*, cyclic voltammetry (CV)) were carried out on single electrodes of similar weight. Anodic and cathodic sweeps were performed by

increasing the overpotential by 0.1 V and monitoring the Coulombic efficiency. The threshold for the definition of the potential limits (*i.e.*, the voltage window) was set at 99.0% efficiency. At these two limits, charge balancing was applied to get the electrodes mass ratio for the optimized devices, m+Q+ = m–Q–. The mass ratio was defined as r+,– = m+/m–. From the experiments (Figure 2), it emerged that the electrolyte could withstand 2.1 V with electrode masses unbalanced by a factor of 1.1.

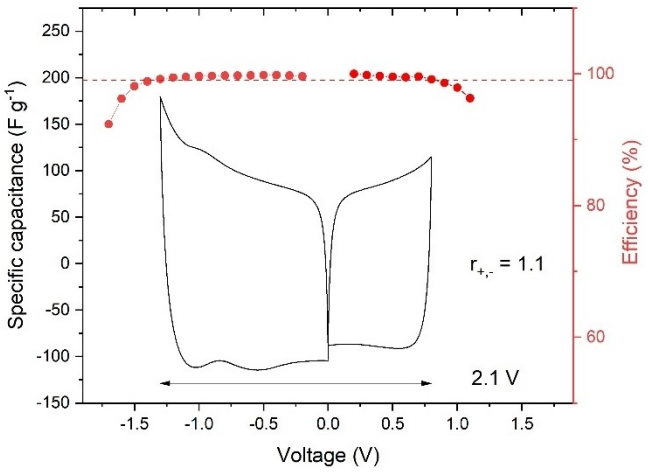

Figure 2. Anodic and cathodic CVs (recorded at 1 mV s^{-1}) for the electrode mass ratio estimation.

Coin cell devices were assembled to run several electrochemical studies. Rate capability tests were run in galvanostatic charge-discharge (GCD) by applying the following current rates: 0.1, 0.2, 0.5, 1.0, and 2.0 A g^{-1}. The results of this test are shown in Figures 3 A and B. In the former, it is possible to observe that the device experienced an initial capacitance loss, as also evidenced by the slightly low Coulombic efficiency and the fast capacitance loss in the very first cycles at the lowest specific current. On the other hand, at 2.0 A g^{-1} the capacitance was retained up to 60% of the initial one, which was an expected result for a EDLC system based on a viscous electrolyte. It is also interesting to observe that, when the test returned to the first specific current value, the capacitance was restored to the previous value. Because of these results, the Ragone plot (shown in Figure 3B) was derived by exploiting – as energy value at 0.1 A g^{-1} – the one derived from the last cycles of the rate capability test. Despite the low voltage window, from the

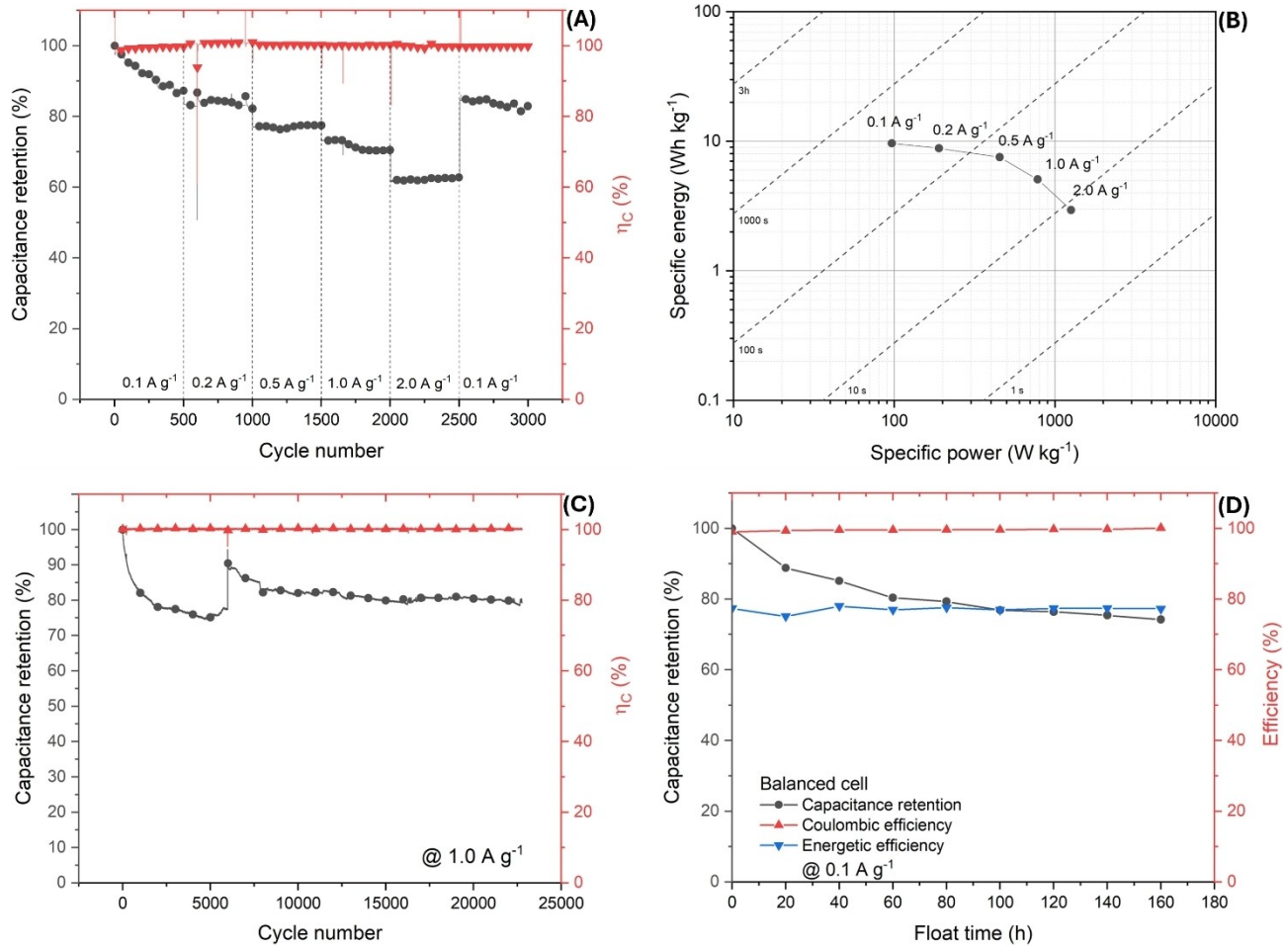

Figure 3. (A) Galvanostatic rate capability test carried out at 0.1, 0.2, 0.5, 1.0, and 2.0 A g^{-1}, showing the capacitance retention and the Coulombic efficiency of the device. **(B)** Ragone plot derived from the rate capability test. **(C)** Capacitance retention derived from a CS test carried out at 1.0 A g^{-1}. **(D)** FT results in terms of capacitance retention, Coulombic, and energy efficiencies.

Ragone plot it can be appreciated that the system showed energy density values greater than 10.0 Wh kg^{-1} at low power densities, while it retained a sufficient energy density (*i.e.*, 3.0 Wh kg^{-1}) at the relatively high-power density value of 2.0 W kg^{-1}.

Aging tests like the standard cycling stability (CS) test and accelerated aging tests (*i.e.*, the float test (FT)) were run to study the system endurance. The results are reported in Figures 3C and D, respectively. CS was run at 1.0 A g^{-1}. It can also be observed, in this case, a quite fast initial capacitance loss, but after 5000 cycles the device retained its capacitance almost constantly with remarkable stability in the Coulombic efficiency values. This remarkable stability can be also observed from the FT results shown in Figure 3D. This test was run by alternating 50 GCD cycles at 0.1 A g^{-1} with 20 h of constant voltage retention periods. Again, the device showed an initial capacitance loss of 10 % of its initial value, after which the aging time constantly reduced. What is also interesting to observe is the overall energy efficiency of the device, which remained almost constant above 75 %.

The reported results are quite encouraging: despite the reduced operative voltage with respect to conventional solvents,[21] the GlyC-based device showed an average specific energy in the field of EDLCs.[35] Concerning the power capabilities, these are slightly reduced with respect to high power EDLC systems because of the overall electrolyte conductivity. In possible future developments, GlyC can be investigated diluted in a less viscous solvent to improve the conductivity.

Solketal Carbonate for Potassium Batteries Electrolyte

The rapidly growing field of KIBs is now exploring new electrolyte formulations targeting long-term stability, low-cost, use of solvents coming from oil-alternatives, understanding salt molarity/performance correlation.[36] In this work, we explored the positive effect of SLC as an additive for the commonly used liquid electrolyte based on potassium hexafluorophosphate (KPF_6) salt 0.8 M in a ethylene carbonate:diethyl carbonate (EC:DEC) mixture; its electrochemical behavior was compared with that of cells assembled with the reference liquid electrolyte (*i.e.*, SLC-free).

As a starting step, it was checked how much the SLC addiction affected the ionic conductivity of the EC:DEC-based liquid electrolyte. This latter figure of merit expresses the ability of the electrolyte to conduct potassium ions through the separator thickness and must be kept as high as possible. Figure 4A shows that the ionic conductivity of the standard electrolyte was higher than that of the SLC-additivated formulation in the whole temperature range. Anyway, this difference was rather little (*i.e.*, ionic conductivity values remained in the 10^{-3} S cm^{-1} order of magnitude in both cases) and became lower at higher temperatures, when the viscosity of the SLC-based electrolyte decreased, as shown in Figure 4B.

The voltage upper limit of the proposed electrolyte is tested in a symmetrical cell consisting of the impregnated separator

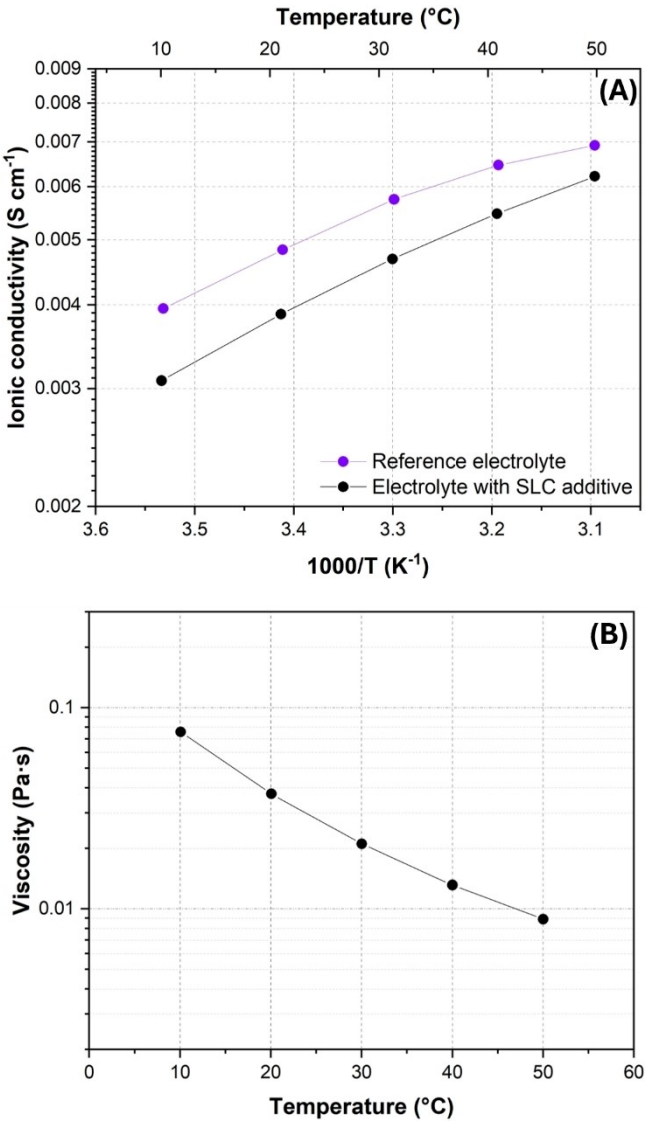

Figure 4. (**A**) Ionic conductivity values of reference and SLC-based electrolytes in the temperature range from 10 to 50 °C. (**B**) Viscosity measurements in the same temperature range for an electrolyte formulated with KPF_6 0.8 M in a SLC-based EC:DEC mixture.

sandwiched between two stainless steel plates by a linear sweep voltammetry experiment. The increase of the current, shown in Figure 5, is noticeable only from potentials higher than 3.8 V, proving its feasibility as electrolyte for our case study on potassium-metal batteries.

The electrochemical performances of the SLC-based liquid electrolyte were tested in half-cells assembled by interfacing a potassium metal anode with a carbon-based cathode; results are shown in Figure 6B and compared with those of a half-cell assembled with a standard liquid electrolyte (Figure 6A). With respect to the results of the reference electrolyte, the cell assembled with the proposed electrolyte reached lower specific capacities, but showed overall identical Coulombic efficiencies and, after 200 cycles, still shows a rather stable electrochemical behavior. In any case, the experiment already carried out on laboratory-scale prototypes has shown that it is possible to use

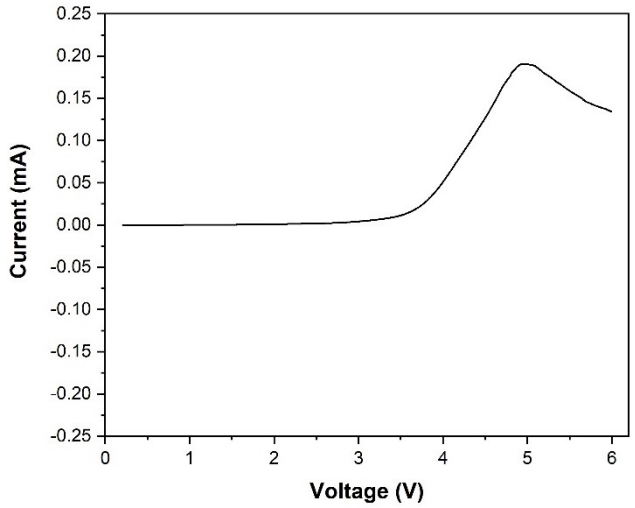

Figure 5. Linear sweep voltammetry response of SLC-based electrolytes from its open-circuit voltage (OCV) to 6 V.

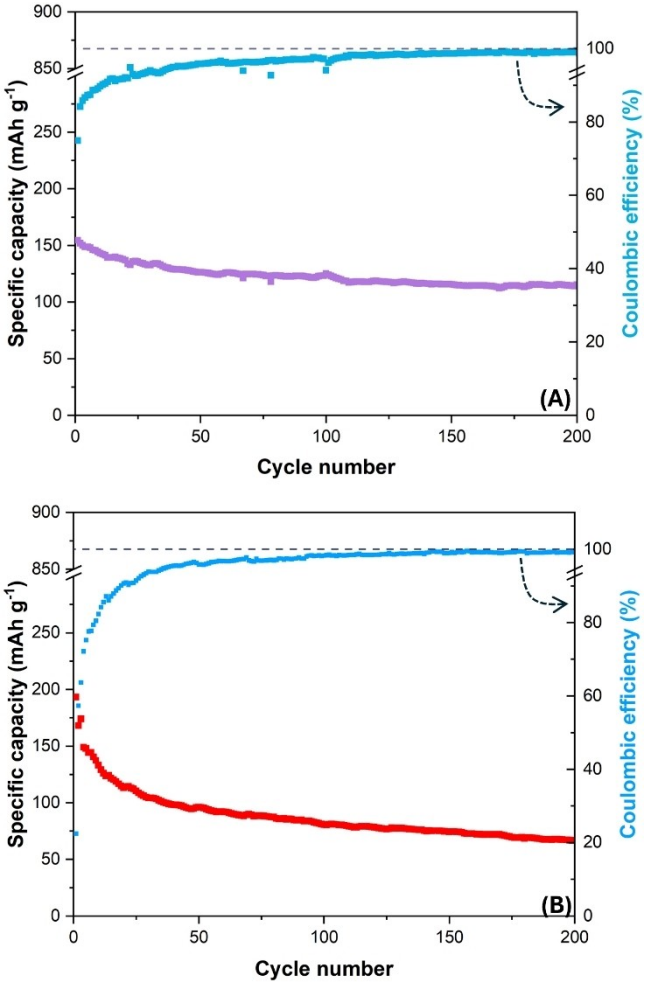

Figure 6. Charging cycles at constant current density of 0.05 A g^{-1} and related Coulombic efficiency of half-cells assembled interfacing potassium metal *vs* Super P carbon and using a (**A**) reference electrolyte and a (**B**) SLC-based electrolyte.

glycerochemistry-derived products for the formulation of secondary batteries electrolytes; considering the important volumes that will be produced when these technologies will be exploited at a large scale to store electricity from renewable sources, it is essential to be able to count on low-impact compounds, not derived from petrochemicals.

Conclusions

Biobased GlyC and SLC derived from glycerol have been synthesized and characterized for their feasibility as suitable chemicals for the preparation of electrolytes in EDLCs and KIBs, respectively.

Electrochemical characterization showed that both compounds are promising for the fabrication of electrochemical energy storage devices. In the case of EDLCs, the electrolyte formulated with GlyC guaranteed excellent performance even adopting very long testing protocols (*i.e.*, more than 20 000 cycles). As regards KIBs, the performance of the cells assembled with the SLC-based electrolyte was not exceptional, but the assembled prototypes were able to complete the charge/discharge testing protocol reaching 200 cycles without particular issues. Concerning this potassium-based energy storage technology, it is imperative to delve deeper into additional glycerochemistry-derived compound families, both as additives to electrolytes and as solvents, with the objective of enhancing electrochemical performance.

Overall, this work has highlighted the possibility of assembling both high energy and high power energy storage devices based on sustainable and no-toxic chemicals obtained from glycerol, *i.e.* the main by-product of the biodiesel industry. To this purpose, our laboratories are now exploring additional molecules to be used in mixtures or as alternatives to the compounds presented in this work, to maximize both performance and circularity of batteries and supercapacitors.

Experimental Section

Chemicals and Materials

Glycerol (99.5%), dimethyl carbonate (DMC, 99%), solketal (1,2-isopropylideneglycerolsodium carbonate, 97%), sodium carbonate (99.5%), CH_3ONa (99%), EC (99%), DEC (99%), dichloromethane (CH_2Cl_2, 99%), KPF_6 (99.5% trace metals basis), Whatman glass fiber (grade D), poly(tetrafluoroethylene) (PTFE, 60 wt% suspension in water), N-methyl-2-pyrrolidone (NMP), and potassium (cubes in mineral oil, 99.5% trace metals basis) were purchased from Sigma-Aldrich. Conductive carbon Super P and polyvinylidene fluoride (PVDF) were purchased from Alfa Aesar. Activated carbon (AC) powder was the commercial product YP-50 F, provided by Kuraray. Carbon black (CB) C65 was provided by Imerys, while sodium carboxymethyl cellulose (CMC) was provided by MTI corp. $TEABF_4$ was provided by IoLiTec. Aluminium foils were provided by S4R, while copper

ones from CIVEN Metal. All chemicals were used without any further purification.

Glycerol Carbonate Preparation, Characterization, and Testing

GlyC was synthesized by glycerol transesterification with dimethyl carbonate in the presence of Na_2CO_3 as catalyst and characterized by means of ^1H and ^{13}C nuclear magnetic spectroscopy (see supporting information), as reported in our previous work.[32] The GlyC-based electrolyte (and the devices described below) were prepared in a N_2-filled glove box, with $O_2 < 0.5$ ppm and $H_2O < 0.5$ ppm.

$TEABF_4$ was chosen as a salt and its solubility in GlyC was determined by evaporating the solvent blandly from a sample of saturated solution (5 mL) and weighing the precipitated salt. $TEABF_4$ solubility was determined to be 1.45 M at 25 °C, but a concentration equal to 1.0 M will be used in this work to ease the comparison with other literature papers where this molarity is commonly adopted. In the subsequent experiments, 1.0 M solution in GlyC was heated at 60 °C and mixed with vortex to fasten the electrolyte dissolution process.

AC-based electrodes were prepared according to the following procedure. 85 wt% of AC, 10 wt% of CB, and 5 wt% of CMC were mixed in deionized water (DIW) at the following ratio: 0.1 mL H_2O per mg CMC. DIW was preheated at 60 °C prior to the binder dissolution and stirring. CB was added to the hot solution and let uniformly disperse while stirring. AC powder was added in several tranches to let the stirring solution get a homogenous composition, then the heating plate was removed, and the final slurry was stirred overnight.

The slurry was doctor-bladed on battery-grade aluminium with a wet thickness of 150 μm. The slurry was let dry overnight before the electrode was cut. The cut electrodes were dried in a Büchi dry oven at 120 °C under high vacuum conditions provided by a rotary pump. The mass loading was 2 mg cm^{-2}.

Self-standing carbon electrodes were prepared to be exploited as the counter electrode (CE) and pseudo-reference electrode. 85 wt% AC, 10 wt% CB, and 5 wt% PTFE were mixed in excess ethanol and let stir at 60 °C. The solution was stirred until the powders agglomerated in a uniform dough phase. The obtained material was flattened and cut when slightly wet. The electrodes were properly dried in Büchi dry oven according to the same procedure used for the EDLC electrodes. The mass loading was 2 mg cm^{-2}.

The rheological properties of the studied electrolytes were measured by an Anton Paar MCR 302 rheometer. The measurements were carried out in the temperature range 0–80 °C with temperature steps of 10 °C at a constant shear rate of 1000 s^{-1}.

The electrolyte ionic conductivity was measured in the temperature range 20–100 °C with temperature steps of 20 °C in a Memmert UN32 oven. The conductivity probe was a small volume (0.75 mL) conductivity cell provided by Amel.

Electrochemical measurements were carried on with VMP3 potentiostat provided by Biologic. Long galvanostatic tests, CS, and rate capability tests, as well as FT, were run using a BT2000 testing equipment provided by Arbin Instruments. Whatman glass fiber was used as a separator in all the assembled electrochemical cells.

CV measurements were performed to evaluate the cell design parameter, that is, the electrode mass ratio to exploit the full electrolyte voltage window. CVs for the cell design were run at 1 mV s^{-1} with 0.1 mV resolution and the electrode potential was increased by 100 mV after 20 cycles to monitor the evolution of the Coulombic efficiency. The three-electrodes measurements were performed versus carbon pseudo-reference and the CE was a bulky, self-standing carbon electrode. CVs on devices were run at 10 mV s^{-1} to check the response of the device under potentiostatic cycling. The voltage resolution was 0.1 mV.

Electrochemical impedance spectroscopy (EIS) was performed to check cells and single electrode interfacial properties. EIS measurements were performed in the 10^6–10^{-2} Hz frequency range, with a probe signal amplitude of 5 mV. The voltage resolution was 0.1 mV and each frequency point was averaged over 3 periods.

Galvanostatic cycles were implemented to test cycling stability and to check the capacitance retention during float tests. CS tests were run in the device voltage window at 1.0 A g^{-1}. Float tests were implemented by alternating 50 galvanostatic cycles run at 0.1 A g^{-1} with constant voltage floating periods of 20 h at the rated voltage. Rate capability tests were run by applying the cell to several current rates: 0.1, 0.2, 0.5, 1.0, 2.0 A g^{-1}.

Three-electrodes measurements were run in PFA Swagelok-type cells. The contacts were made of AISI 316 L, covered by poly(ether ether ketone) in the cell proximities. The cells were assembled with a poly(imide) layer covering the cell walls and alloying the pseudo-reference to contact the cell solution.

Device measurements were carried out in a 2032 coin cell setup. The cells were assembled with standard AISI316 L spacers and springs. The cell stacks were assembled with two 0.5 mm spacers and a spring.

Solketal Carbonate Preparation, Characterization, and Testing

SLC was prepared by reacting solketal and DMC in the presence of sodium methoxide as catalyst (see supporting information).[33] Electrochemical characterization tests were carried out on electrochemical potassium-based cells using commercial materials for electrodes and electrolytes, the performances of which are thus already established, and adding the newly proposed SLC compound into the electrolyte to investigate its effect on the electrochemical behavior.

The commercial liquid electrolyte was KPF_6 0.8 M in EC:DEC (50:50, v/v), used as a reference electrolyte, while the proposed formulation was based on KPF_6 0.8 M in EC:DEC:SLC (47.5:47.5:5, v/v). KPF_6 0.8 M in SLC was used for the rheological analysis. Both electrolyte solutions were tested in electrochemical cells, by wetting a glass microfiber separator (Whatman, 18 mm of diameter, 0.65 mm of thickness) placed between cell electrodes.

For all the electrochemical characterization tests, two cell configurations were used: i) half-cells were assembled in 2032 coin architecture, using potassium foil as anode and Super P-coated copper discs as cathode, separated by the wetted glass microfiber separator; ii) a symmetrical configuration with a soaked separator pressed between two stainless steel plates in ECC-Std cell (EL-CELL). All the configurations were assembled in an argon-filled glove box ($O_2 < 0.5$ ppm and $H_2O < 0.5$ ppm).

Electrodes were fabricated by mixing the conductive carbon Super P and the PVDF binder at a weight ratio of 80:20. NMP was added until a homogeneous paste was obtained. The resulting slurry was ball milled at 30 Hz in a Retsch MM 400 equipment, then casted on a copper foil by doctor blade technique, by using a 200 μm-thick blade and an automatic film applicator (Sheen) at a speed of 50 mm s^{-1}. The deposited paste was dried at 40 °C for 2 h. Disks of 15 mm diameter were cut by a manual cut and dried at 120 °C under vacuum for 4 h. The mass loading was ca. 0.9 mg cm^{-2}.

Symmetrical cells were used to measure the ionic conductivity of the commercial and the newly proposed electrolyte. By means of a digital controlled climatic chamber (MK 53 E2.1, BINDER), the temperature of the ECC-Std cell was decreased from 50 to 10 °C (with a step of 10 °C) and rested at each temperature to perform – after 1 h – an EIS measurement. The latter was conducted in the frequency range between 100 kHz and 10 mHz, at the oscillating potential of 10 mV, and allowed to obtain the electrolyte resistance (R_b) value and, thus, the ionic conductivity (σ) through the following equation:

$$\sigma = L/(Rb \cdot S) \quad (1)$$

where L is the activated separator thickness and S is its surface area.

A linear sweep voltammetry was carried out on an ECC-Std cell, assembled according to symmetrical configuration (*i.e.*, the Whatman glass fiber impregnated with the newly conceived electrolyte sandwiched between two stainless steel plates). The cell potential was increased from its almost null OCV to 6 V at a scan rate of 0.1 mV s^{-1}, and the current response was recorded by the potentiostat.

The performance assessment was carried out by charging and discharging between 0.01 and 3 V the half-cell configuration at the fixed current density of 0.05 A g^{-1} of SuperP active mass for 50 cycles. The galvanostatic charging and discharging tests were performed on an Arbin battery cycler instrument at room temperature.

Supporting Information Summary

Additional supporting information can be found online in the Supporting Information section at the end of this article.

Acknowledgments

These results are part of a project that has received funding from the European Research Council (ERC) under the European Union's ERC Starting Grant agreement "CO2CAP" No. 949916. This work was also partially funded by the project "nuovi Concetti, mAteriali e tecnologie per l'iNtegrazione del fotoVoltAico negli edifici e in uno scenario di generazione diffuSa" ("CANVAS"), funded by the Italian Ministry of the Environment and the Energy Security, through the Research Fund for the Italian Electrical System (type-A call,published on G.U.R.I. n. 192on18-08-2022). This study was also carried out within the MOST – Sustainable Mobility Center and received funding from the European Union Next-GenerationEU (PIANO NAZIONALE DI RIPRESA E RESILIENZA (PNRR) - MISSIONE 4 COMPONENTE 2, INVESTIMENTO 1.4 - D.D. 1033 17/06/2022, CN00000023). Finally this research work has also been supported also by the "Progetto Orangees - ORgANics for Green Electrochemical Energy Storage - codice CSEAA 00010" funded by the Italian Government through the MITE (Ministero della Transizione Ecologica) call 2022 "Bandi di gara di tipo A". This work was also funded by research fund "FARB", University of Salerno (ORSA211701). Open Access publishing facilitated by Università degli Studi di Salerno, as part of the Wiley - CRUI-CARE agreement. This study was carried out within the «GREEN2-MOVE» project [FISA-2022-00983] funded by Ministero dell'Università e della Ricerca (Bando FISA 2022). Open Access publishing facilitated by Università degli Studi di Salerno, as part of the Wiley - CRUI-CARE agreement.

Conflict of Interests

The authors declare no conflict of interest.

Data Availability Statement

The data that support the findings of this study are available from the corresponding author upon reasonable request.

Keywords: Glycerol carbonate · Solketal carbonate · Potassium battery · Supercapacitor · Electrolyte.

[1] R. Cucciniello, P. T. Anastas, *Curr. Opin. Green Sustainable Chem.* **2021**, *31*, 100528.
[2] J. B. Zimmerman, P. T. Anastas, H. C. Erythropel, W. Leitner, *Science* **2020**, *367*, 397–400.
[3] F. D. Monica, M. Ricciardi, A. Proto, R. Cucciniello, C. Capacchione, *ChemSusChem* **2019**, *12*, 3448–3452.
[4] P. T. Anastas, J. C. Warner, *Green Chemistry: Theory and Practice*, Oxford University Press, Oxford, UK **1998**.
[5] P. Prete, D. Cespi, F. Passarini, C. Capacchione, A. Proto, R. Cucciniello, *Curr. Opin. Green Sustainable Chem.* **2022**, *35*, DOI 10.1016/j.cogsc.2022.100624.
[6] M. Pagliaro, R. Ciriminna, H. Kimura, M. Rossi, C. Della Pina, *Angew. Chem. Int. Ed.* **2007**, *46*, 4434–4440.
[7] M. Itatani, N. Német, N. Valletti, G. Schuszter, P. Prete, P. Lo Nostro, R. Cucciniello, F. Rossi, I. Lagzi, *ACS Sustainable Chem. Eng.* **2023**, *11*, 13043–13049.

[8] A. A. F. da Costa, A. de N. De Oliveira, R. Esposito, C. Len, R. Luque, R. C. R. Noronha, G. N. Da Rocha Filho, L. A. S. Do Nascimento, *Catalysts* **2022**, *12*, 570.
[9] M. Sutter, E. D. Silva, N. Duguet, Y. Raoul, E. Métay, M. Lemaire, *Chem. Rev.* **2015**, *115*, 8609–8651.
[10] R. Gérardy, D. P. Debecker, J. Estager, P. Luis, J.-C. M. Monbaliu, *Chem. Rev.* **2020**, *120*, 7219–7347.
[11] D. Cespi, R. Cucciniello, M. Ricciardi, C. Capacchione, I. Vassura, F. Passarini, A. Proto, *Green Chem.* **2016**, *18*, 4559–4570.
[12] G. Piana, M. Ricciardi, F. Bella, R. Cucciniello, A. Proto, C. Gerbaldi, *Chem. Eng. J.* **2020**, *382*, 122934.
[13] S. Wang, L. Lyu, R. Farnood, N. Yan, *Mater. Today Sustainability* **2020**, *9*, 100038.
[14] N. M. J. Rasali, A. S. Samsudin, *Ionics* **2018**, *24*, 1639–1650.
[15] H. Guo, C. Wang, *ChemSusChem* **2024**, *17*, e202301586.
[16] H. Liao, H. Chen, F. Zhou, Z. Zhang, *J. Mater. Sci.* **2020**, *55*, 9504–9515.
[17] S. Wang, P. Xiong, J. Zhang, G. Wang, *Energy Storage Materials* **2020**, *29*, 310–331.
[18] J. Liu, S. Min, F. Wang, Z. Zhang, *J. Power Sources* **2020**, *466*, 228347.
[19] J. Liu, S. Min, F. Wang, Z. Zhang, *Energy Technol.* **2020**, *8*, 2000391.
[20] Z. Lin, E. Goikolea, A. Balducci, K. Naoi, P. L. Taberna, M. Salanne, G. Yushin, P. Simon, *Mater. Today* **2018**, *21*, 419–436.
[21] L. H. Hess, A. Balducci, *Electrochim. Acta* **2018**, *281*, 437–444.
[22] A. Scalia, P. Zaccagnini, M. Armandi, G. Latini, D. Versaci, V. Lanzio, A. Varzi, S. Passerini, A. Lamberti, *ChemSusChem* **2021**, *14*, 356–362.
[23] H. Tan, X. Lin, *Molecules* **2023**, *28*, 823.
[24] L. Duan, H. Tang, X. Xu, J. Liao, X. Li, G. Zhou, X. Zhou, *Energy Storage Mater.* **2023**, *62*, 102950.
[25] P.-F. Cao, B. Li, G. Yang, S. Zhao, J. Townsend, K. Xing, Z. Qiang, K. Vogiatzis, A. Sokolov, J. Nanda, T. Saito, *Macromolecules* **2020**, *53*, 3591–3601.
[26] M. W. Logan, S. Langevin, B. Tan, A. W. Freeman, C. Hoffman, D. B. Trigg, K. Gerasopoulos, *J. Mater. Chem. A* **2020**, *8*, 8485–8495.
[27] P. Zaccagnini, Y. Tien, L. Baudino, A. Pedico, S. Bianco, A. Lamberti, *Adv. Mater. Technol.* **2023**, *8*, 2300833.
[28] C. Zhao, F. Ding, H. Li, S. Zhang, X. Liu, Q. Xu, *Ionics* **2020**, *26*, DOI 10.1007/s11581-020-03720-4.
[29] F. P. Nkosi, M. Valvo, J. Mindemark, N. A. Dzulkurnain, G. Hernández, A. Mahun, S. Abbrent, J. Brus, L. Kobera, K. Edström, *ACS Appl. Energy Mater.* **2021**, *4*, 2531–2542.
[30] T. Tabanelli, C. Giliberti, R. Mazzoni, R. Cucciniello, F. Cavani, *Green Chem.* **2019**, *21*, 329–338.
[31] M. O. Sonnati, S. Amigoni, E. P. T. de Givenchy, T. Darmanin, O. Choulet, F. Guittard, *Green Chem.* **2013**, *15*, 283–306.
[32] N. Valletti, M. Acar, R. Cucciniello, C. Magrini, M. A. Budroni, D. Tatini, A. Proto, N. Marchettini, P. Lo Nostro, F. Rossi, *J. Mol. Liq.* **2022**, *357*, 119114.
[33] J. A. Kenar, G. Knothe, *J. Americ. Oil Chem. Soc.* **2008**, *85*, 365–372.
[34] M. Ricciardi, L. Falivene, T. Tabanelli, A. Proto, R. Cucciniello, F. Cavani, *Catalysts* **2018**, *8*, 391.
[35] J. Libich, J. Máca, J. Vondrák, O. Čech, M. Sedlaříková, *J. Storage Mater.* **2018**, *17*, 224–227.
[36] C.-H. Jo, S.-T. Myung, *Adv. Energy Mater.* **n.d.**, *n/a*, 2400217.

Manuscript received: July 24, 2024
Accepted manuscript online: August 16, 2024
Version of record online: October 18, 2024